ISSN 1392–1320 MATERIALS SCIENCE (MEDŽIAGOTYRA). Vol. 17, No. 4 2011

Structure, Properties and Applications of Diamond Like Nanocomposite (SiO_x Containing DLC) Films: A Review

Šarūnas MEŠKINIS *, **Asta TAMULEVIČIENĖ**

Institute of Materials Science of Kaunas University of Technology, Savanorių av. 271, Kaunas LT-50131, Lithuania

crossref http://dx.doi.org/10.5755/j01.ms.17.4.770

Received 14 September 2011; accepted 02 November 2011

The present article reviews current situation on SiO_x containing diamond like carbon (diamond like nanocomposite) films. The overview of different deposition methods and reagents used is presented; chemical composition of different diamond like nanocomposite films is described. Different models of structure of diamond like nanocomposite films are considered. Mechanical, optical, electrical properties as well as surface energy of diamond like nanocomposite films produced by different methods are reviewed and discussed. The survey of different potential and industrial applications of diamond like nanocomposite films is presented.

Keywords: SiO_x containing diamond like carbon, diamond like nanocomposite films.

1. INTRODUCTION

Diamond-like carbon (DLC) is an umbrella term that refers to different forms of amorphous carbon materials that display some of the unique properties of natural diamond [1, 2]. DLC is a mixture of sp^2 and sp^3 bonded carbon atoms – some kind of the composite material consisting of the sp^2 bonded (graphite like) carbon clusters embedded into the sp^3 bonded carbon (diamond like) matrix. Hydrogen can be present in these films with an atomic concentration between 0 % and up to 50 %. The DLC acronym was introduced by Aisenberg and Chabot [1] who for the first time have produced amorphous carbon films exhibiting many of the properties of diamond and have stimulated current interest to this field. Due to the room temperature deposition possibility, no limitation of materials (the various forms of DLC can be applied to almost any material that is compatible with vacuum environment), ultrasmooth surface (roughness less than few nm), uniform large area deposition (providing high productivity and low cost), unique and tunable properties of the material (high hardness (10 GPa – 80 GPa)); low friction and high wear resistance; chemical inertness; optical transmittance (transparency for visible and infrared light (60 % – 90 %); good thermal conductivity (4 – 18 W/cmK); radiation resistance as well as control of the electrical resistivity in very wide range, these films find many applications ranging from “data to beer storage” [2, 3]. At the moment achievements in this field and technology of DLC can be described as a matured technology with global competency. Most of the present industrial applications of DLC can be considered in the category protective coatings [2 – 5].

Along with the change of the sp^3 and sp^2 bonded carbon ratio and hydrogen content, properties of the DLC films can be further controlled by doping them with different chemical elements or compounds. Particularly SiO_x containing diamond like carbon films (DLC:SiO_x), otherwise diamond like nanocomposites (DLN), were developed in the early 1990s [6]. DLC:SiO_x films received considerable interest due to the substantially reduced stress level, increased thermal stability, high hardness, low friction. Hydrophobicity of the DLN films is comparable with that of Teflon. Dielectric permittivity and refractive index of SiO_x containing DLC is lower than in the case of the undoped DLC and comparable with those of SiO_2, while optical transparency is higher.

This review summarizes studies done on deposition, structure, chemical composition as well as mechanical, optical, electrical, hydrophobic properties of DLC:SiO_x films. Industrial and prospective applications of SiO_x containing DLC films are considered.

2. SYNTHESIS OF DLC:SiO_x FILMS: DEPOSITION METHODS AND REAGENTS

Radio frequency (RF) capacitively coupled (CCP) plasma enhanced chemical vapour deposition (PECVD) was the most often used DLC:SiO_x deposition method (eg., see [7 – 15]. Application of the pulsed DC CCP PECVD [16], inductively coupled plasma (ICP) PECVD [17 – 20], hot filament assisted PECVD [21 – 26], deposition by closed drift (anode layer) ion beam source (CDIBS) [27 – 37], Kaufman ion source [38] and electron cyclotron wave resonance (ECWR) plasma beam source [16, 39 – 41] was reported by different researchers as well. It seems, that such a widely used DLC and metal containing DLC deposition methods as arc evaporation, sputtering and laser ablation are rarely used for synthesis of the DLC:SiO_x. Only in [42] ion beam sputtering of Si/SiO_2 target assisted by hydrocarbon ion beam irradiation was used for growth of SiO_x containing DLC film.

DLC:SiO_x films can be synthesized using different silicon and oxygen containing precursors. These precursors might be gaseous (silane (SiH_4) and oxygen (O_2) mix [43]; tetramethyl silane – TMS ($(CH_3)_3SiH$) and O_2) mix [18]) or liquids (hexamethyldisiloxane-HMDSO ($C_6H_{18}OSi_2$) [7, 17, 39, 40, 44 – 46], tetraethylorthosilicate-TEOS ($SiC_8H_{20}O_4$) [8, 16, 46 – 47], hexamethyldisilane-HMDS ($C_6H_{18}Si_2$) [9 – 10], mixed siloxane and silazane precursors

---

[*] Corresponding author. Tel.: +370-37-313432; fax.: +370-37-314423.
E-mail address: *sarunas.meskinis@ktu.lt* (Š. Meškinis)

[10]). The liquid precursors are more frequently used because of easier handling of the material and variety of choices. Usually the carbon, silicon and oxygen containing vapor is mixed with hydrocarbon gas (methane (CH_4) [8, 45 – 46], acetylene (C_2H_2) [18]) or transported employing argon (Ar) [16], hydrogen (H_2) [27 – 28], helium (He) [28 – 29], oxygen (O_2) [43] gases and etc. Depending on the selection of the precursor, one can get different final composition of the films. Single gaseous precursor mentioned above (SiH_4) is known to be highly flammable and the care must be taken when it is mixed with oxygen during deposition. HMDSO is the most frequently used precursor. The reasons are probably easy usage of HMDSO because of low toxicity and flammability and its high versatility allowing to produce different types of materials [7, 17, 39, 44 – 45]. It serves as a precursor for C, H, Si and O. HMDSO can be vaporized in room temperature. The mentioned precursors with main characteristics are listed in Table 1.

Table 1. Precursors used in DLC:SiO_x films formation

Precursor	Formula	Mol. weight, g/mole	Boiling point, °C	Physical state
HMDSO	$C_6H_{18}OSi_2$	162.38	101	Liquid
HMDS	$C_6H_{18}Si_2$	146.38	112	Liquid
TEOS	$SiC_8H_{20}O_4$	208.33	168	Liquid
Silane	SiH_4	32	–111	Gas
TMS	$(CH_3)_3SiH$	74.2	6.7	Liquified gas

3. STRUCTURE AND CHEMICAL COMPOSITION

The most common techniques used for investigation of the structure and composition of DLC and DLN films are Raman spectroscopy, Fourier Transformed Infrared Spectroscopy (FTIR) and X-ray Photoelectron Spectroscopy (XPS). Combination of these techniques gives comprehensive information about the chemical composition and bonds in these films.

3.1. Chemical composition

Employing XPS one can determine the surface composition of the films. In DLC films, the carbon core C 1s spectra consists of peaks due to sp^3 (285.2 eV) and sp^2 (284.4 eV) bonded carbon, CO-contaminants (286.5 eV) and SiC (283.7 eV) phases. The trace of Si results from the internal sputtering of Si atoms, travelling back through the carbon layer and accumulating on the surface during deposition [48]. The area of each peak is directly related to the concentration of the corresponding phase [49].

It was found that DLC:SiO_x films consist of carbon, silicon and oxygen, yet it is not possible to determine amount of the hydrogen by XPS technique. Analysing the shape and position of the peaks attributed to the C, Si and O one can determine bonding (C–C, Si–C, O–C–O, Si–O) [8], and quantitative information might be obtained. It was observed that C 1s spectra exhibits nearly symmetric shape centred at around 285.4 eV which was assigned to C–C bonds in carbon matrix in the film [8]. Sometimes additional features (like in DLC) might be observed in the spectra such as Si–C (283 eV), or O–C–O (288.6 eV). Identification of chemical environment can be relatively straightforward for carbon, where the C 1s core level has clearly defined features. In the case of silicon, binding energy shifts in the Si 2p core level cover range of only 4 eV. Therefore, it is often difficult to resolve distinct features by curve-fitting the Si 2p core level [50]. Assumptions were made that all Si atoms in DLC:SiO_x have a valence of four. The major factor in determining the Si 2p binding energy is the number of oxygen atoms bound to the Si atom. A secondary effect upon the Si 2p binding energy is the various combinations of C and H atoms fulfilling the remaining bonding requirements of silicon, i. e. –H, –CH_2-, =CH_2, –CH=CH–, –CH=CH_2, –CH_3 and –CH_2–O– [51]. These bonding configurations may induce shift of the Si 2p binding energy, which is very small compared with the shift caused by oxygen [51]. According to [50] and [51] there could be only four component peaks within the Si 2p envelope: 1) a peak at (101.5 ±0.1) eV, which can be attributed to $(CH_3)_3SiO$ units, 2) at (102.1 ±0.1) eV due to $(CH_3)_2SiO_2$ units, 3) at (102.8 ±0.1) eV, which can be assigned to CH_3SiO_3 units and 4) at (103.4 ±0.1) eV due to SiO_4 units.

In the case of DLC:SiO_x deposition from TEOS, it was observed that amount of Si in the films has influence on the position of the Si 2p peak [16]. At small silicon concentrations (<5 at.%), Si 2p envelope can be approximated by two peaks at (101.6 ±0.4) eV (attributed to $(CH_3)_3SiO$ units) and (102.5 ±0.3) eV (attributed to the polymeric siloxane structures). Increasing concentration of silicon, the Si 2p peak is approximated by single peak, and the position of this peak shifts from (102.2 ±0.2) eV (9 at.% – 13 at.%) to (102.9±0.1) eV (22 at.%). These shifts indicate that at small Si concentrations silicon is present in siloxane structures with transition to silsesquioxane bonding at higher concentrations [16, 46]. Otherwise, when films are formed from HMDSO the C–Si–O–Si–C molecular fragments were the major building blocks in the film [40]. In the case of films formed from HMDSO/H_2, the Si 2p peak was analyzed as superposition of SiC and SiO_x ($x < 2$) components [27]. It was also observed that using O_2 gas during deposition the fraction of a-SiO_x phase increases (increasing O_2 amount in plasma) with decrease of a-C:H phase [43]. At low O_2 fractions, silicon atoms are incorporated into the DLC phase bonded to carbon. However, when the O_2 fraction is increased phase segregation is expected to take place, since Si–O bonds would be favoured compared to Si–C or C–O bonds [43]. From the XPS results one can obtain a conclusion that using most common precursors (TEOS, HMDSO, $CH_4/SiH_4/O_2$), the structure of the obtained films consists of two amorphous phases: first one – rich in carbon and hydrogen atoms (DLC); the second one – rich in silicon and oxygen atoms (a-SiO_x).

Results obtained from the FTIR and XPS analysis give further insight into the chemical bonds existing in the films. In the FTIR spectra of hydrogenated DLC, only bands corresponding to the C–H_x ($x = 2, 3$) bond vibrations situated in the range (2800 – 3100) cm^{-1} are usually observed [47]. Analysing the intensity of these peaks it is possible to determine the sp^3/sp^2 ratio, but the results might be unreliable due to the fact that only the amount of C–H bonds and not C–C bonds is determined and it also depends on the amount of hydrogen in the films [52]. Speaking about IR spectra of DLC:SiO_x films, it predominantly consists of C–C (1558 cm^{-1}), C–H (2850 – 3100 cm^{-1}), Si–C (760 cm^{-1}), Si–H (2320 cm^{-1}), and Si–O (874 cm^{-1}) bonds [8 – 10, 47].

The spectrum of DLC:SiO_x film, formed from HMDSO/H_2 precursor, is presented in Fig. 1.

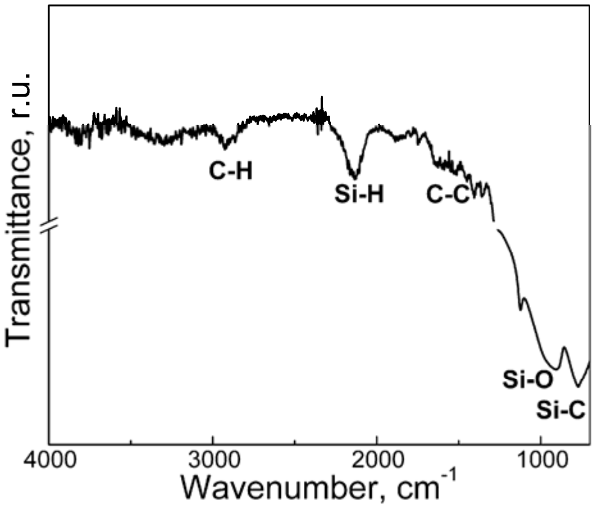

Fig. 1. FTIR spectra of DLC:SiO_x film formed from HMDSO/H_2 by CDIBS

The most intense peak is attributed to the Si–O vibrations, situated around 1000 cm^{-1} [16]. Si-H stretching vibrations at 2320 cm^{-1} [10] observed in FTIR spectra were explained by the idea that some Si atoms are surrounded by some organic environment rather than being incorporated in a SiO_x network [9]. Change of ion beam energy reduces the intensity of this peak [28]. The C–H stretching, like in DLC films, is also important vibration in DLN films. The C–H and Si–O stretching vibrations observed in spectra confirms that films are mainly comprised of the interpenetrating a-C:H and a-Si:O networks [9, 47]. The intensity of the C–H and Si–H peaks can give information about the bound hydrogen in the films [53]. But the most reliable results about hydrogen concentration are obtained using other characterization techniques, such as Rutherford back scattering (RBS) and elastic recoil detection (ERDA). It was reported that DLC:SiO_x films might contain (20 – 47) at.% of hydrogen [7, 21].

3.2. Structure

Raman spectroscopy is a fast and nondestructive tool for characterisation of amorphous carbons as it can give information about the clustering of sp^2 phase, the orientation of sp^2 phase, the H content [54]. All carbons show common features in their Raman spectra in the (800 – 2000) cm^{-1} region, the so-called G and D peaks, which lie at ~1560 cm^{-1} and ~1360 cm^{-1}, respectively, for visible excitation, and the T peak at ~1060 cm^{-1}, which becomes visible only for UV excitation [54]. The G peak is due to the bond stretching of all pairs of sp^2 atoms in both rings and chains. The D peak is due to the breathing modes of sp^2 atoms in rings. The T peak is due to the C–C sp^3 vibrations [8].

Raman spectroscopy was successfully used to analyse DLC:SiO_x films. Raman spectra of these films are similar to those of DLC films: the main feature is broad peak seen in (1100 – 1700) cm^{-1} range [47]. Typical Raman spectra of DLC:SiO_x films formed from HMDSO/H_2 and HMDSO/He is shown in Fig. 2. The positions of characteristic peaks and additional features are summarised in Table 2.

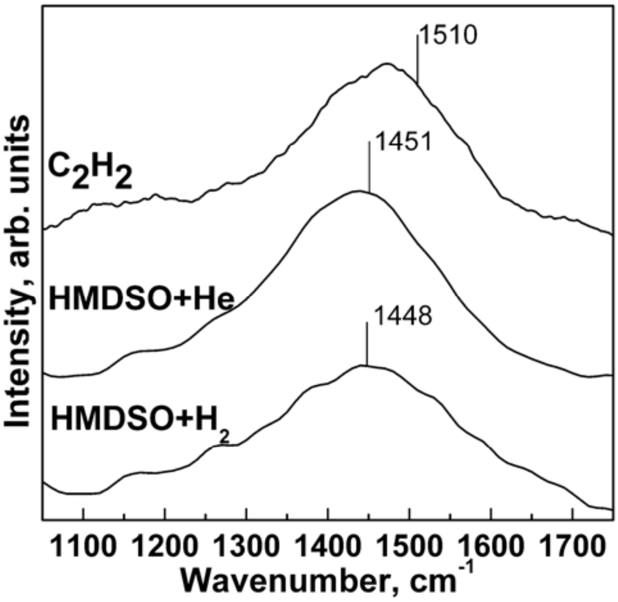

Fig. 2. Raman spectra of the DLC:SiO_x and "conventional" DLC films formed by CDIBS

Numerous authors reported shift of the main Raman scattering peak as well as G peak (fitting component) of the DLC:SiO_x films to the lower wavenumbers in comparison with DLC films [16 – 17, 40, 55]. In [16] it was explained by sensitivity of the position of G peak to the strength of C=C bonds. Incorporation of SiO_x clusters gives substitution of C atoms by heavier Si atoms and weakening of C=C bonds due to the linking of C atoms to more electropositive Si atoms [16]. Yet Si atoms in Si–O bonds are even more electropositive which can lead to additional weakening of C=C bonds [16].

It can be seen in Table 2, that reported G peak (or maximum of the main Raman spectra feature) position was in a very wide range – (1455 – 1544) cm^{-1}. Analysis of the articles where Raman spectra of DLC:SiO_x and DLC films were measured and studied parallely revealed contraversy – in some studies significant shift of the G peak position to the lower wavenumbers was reported [16 – 17, 40, 55], while in other cases the shift was negligible [47, 56]. It seems, that in the case of the films deposited from HMDSO vapor alone or from mixtures of the HMDSO with H_2 or He, shift of the G peak can be large (~60 cm^{-1}) [40, 55]. In these films significant atomic concentrations of Si and O was observed as well (Si 20 % – 25 %, O 16 % – 25%) [27, 36 – 37, 40]. Different results were observed in the case of the DLN films deposited from TEOS – compound with bigger number of the O atoms and smaller number of Si atoms in molecule in comparison with HMDSO one ($C_8H_{20}SiO_4$ vs $C_6H_{18}Si_2O$) (Table 1). In the case of the DLC:SiO_x film deposited from TEOS/H_2/Ar mixture downshift of the G peak was <10 cm^{-1}, while for

Table 2. G peak positions in Raman spectra of DLN and DLC films

	Ref.	G peak (cm^{-1})		Other lines (DLC:SiO$_x$)	Exc. wav., nm
		DLC:SiO$_x$	DLC		
PECVD TEOS/CH$_4$	[8]	~1510*			514.5
CCP PECVD TEOS/CH$_4$	[56]	~1525*	~1525–1530*		
	[13]	~1530*			514.5
DC-PECVD TEOS/Ar	[16]	1530–1540	~1570		514
CCP PECVD TEOS/H$_2$/Ar	[47]	1524, 1526, 1545	1533, 1534, 1538		514.5
PECVD CH$_4$/HMDSO	[17]	1500	1572–1590	1660	514.4
ICP PECVD HMDSO/O$_2$	[20]	1528			514.4
PECVD HMDSO	[9]	1544			514.4
CDIBS HMDSO/H$_2$	[34]	1470*		970–1010, 1120–1150, 1650–1700	532
CDIBS HMDSO/H$_2$	[28]	1450*		1165, 1270, 1450, 1644,	632.8
CDIBS HMDSO/H$_2$	[36]	~1455*		1000	532
CDIBS HMDSO	[37]	1465–1470*		1445	532
CDIBS HMDSO/H$_2$	[55]	1476	1529		532
ECWR HMDSO	[40]	1475*	1535*	1173	488
PECVD, Kaufmann ion source HMDSO	[38]	1520, 1530–1535			514.5
IBAD Si+SiO$_2$ target, C$_2$H$_2$	[42]	1529			514.5

* - position of the main Raman peak maximum.

one sample even some shift of the G peak position to the higher wavenumbers in comparison with Raman spectra of DLC was reported [47]. For DLN films deposited from TEOS/CH$_4$ gas mixture, changes of the G peak position were even smaller in comparison with films synthesized from TEOS/H$_2$/Ar [13, 56]. Yet chemical composition of the film deposited from TEOS/CH$_4$ gas mixture was 57.9 at.% of carbon, 32.8 at.% of oxygen and 9.3 at.% of silicon [13]. While in the case of the films deposited from TEOS/Ar gas mixture even doping by 5 at.% of Si results in downshift of G peak by ~30 cm^{-1} in comparison with the case of DLC [16]. Further increase of the Si atomic concentration up to 22 at.% results in relatively small (but non-monotonic) additional downshift of the G peak position in 10 cm^{-1} range [16]. Such a discrepancy rather contradicts to the theory about the shift of Raman spectra G peak position due to the replacement of C atoms by heavier Si atoms.

Alternative description can be done by taking into account other features observed in Raman spectra of DLC:SiO$_x$ films. In [28, 34, 37, 40] analysing Raman spectra some additional peaks were observed, which can be attributed to the trans-polyacetylene (TPA) chains (see Table 2). Therefore in [28, 37] there were suggested, that shift of the main Raman scattering peak can be explained by appearance of the TPA related peak at ~1450 cm^{-1} besides G and D peaks and the main feature of the Raman spectra of DLC:SiO$_x$ films should be fitted by three peaks instead of two. According to this assumption no real significant shift of G peak position take place in DLN films [28].

In [17] Raman peak around 1660 cm^{-1} was observed. The origin of this peak was explained by the polymeric nature of HMDSO and its tendency to polymerize on the surface as well [17].

In such a way it seems, that in amorphous carbon matrix of DLC:SiO$_x$ films at least in some cases TPA phase present.

In some studies transmission electron microscopy (TEM) and X-ray diffractometry (XRD) were use for search of the possible nanoparticles and crystallites in DLC:SiO$_x$ films. No XRD detectable crystallinity was reported for DLC:SiO$_x$ films deposited by hot filament activated PECVD [26]. Presence of the amorphous SiO$_x$ particles embedded into the amorphous carbon matrix was revealled by HRTEM for DLC:SiO$_x$ films deposited by ICP PECVD, while for DLC:SiO$_x$ films deposited by CCP PECVD no particles was observed [19]. However in [17] crystalline SiO$_x$ nanoclusters were observed in ICP PECVD synthesized DLC:SiO$_x$ films.

4. MECHANICAL PROPERTIES

4.1. Residual stress, hardness and Young's modulus

Internal stress in DLC:SiO$_x$ films is substantially lower than in DLC films. In [19] stress of the DLN films deposited from HMDSO vapour by ICP PECVD was ~1.5 GPa in comparison with 11 GPa of the DLC deposited from CH$_4$ gas. However, stress level as high as 12 GPa was reported for DLC:SiO$_x$ films deposited by lower plasma density CCP PECVD [19]. It was explained by the presence (absence) of the nanoparticles in the case of the DLC:SiO$_x$ films deposited by ICP and CCP PECVD respectively [19]. In [16] stress in DLN film decreased twice with increase of the Si atomic concentration from 0 % to 10 %. At higher Si atomic concentration (>13 at.%) some local increase of the stress was observed. It was explained by formation of the siloxane-bonded DLC networks and SiO$_x$ clusters instead of the siloxane network alone [16]. Internal stress of the DLC:SiO$_x$ films deposited by CDIBS was >2.5 times lower than stress of the DLC films deposited from C$_2$H$_2$ [32]. Due to the decreased stress there is no problem to deposit DLC:SiO$_x$ films thicker than 1 μm, while in the case of the DLC it is problematic. Synthesis of the DLN films of thickness of several microns [7, 11, 21, 43] and even up to 10 μm [12] was reported.

However hardness and Young's modulus decrease for DLC:SiO$_x$ film in comparison with DLC films was reported by numerous authors [7, 8, 12, 14, 16, 18, 56]. The only exception was [19]. Young's modulus of DLC:SiO_x films in all cases was below 160 GPa (see Table 3).

It can be seen in Table 3, that in the case of the CCP PECVD deposited DLC:SiO_x films their hardness exceeded 15 GPa only when CH_4 (hydrocarbon gas) was used as transporting gas along with the siloxane based vapour (HMDSO, TEOS) [7 – 8, 11, 13]. It seems, that in these films content of the SiO_x phase is substantially lower in comparison with ones deposited from the siloxane based vapour alone or HMDSO/Ar (TEOS/Ar) mixture (comparing data from [7, 13, 16,] and [12]). In the case of the ICP PECVD deposited DLN film relatively very high hardness (25 GPa – 30 GPa) equal to the hardness of DLC films deposited from methane alone was reported in [19]. Such a high hardness was explained by formation of the SiO_x nanoparticles in DLN films, while no nanoparticles was found in DLC:SiO_x films deposited by CCP PECVD [19]. However in [17] hardness of ICP PECVD synthesized DLC:SiO_x films was in 12 GPa – 16 GPa range despite presence of the crystalline SiO_x nanoclusters. It should be mentioned, that increase of the plasma density (ion/neutral ratio) results in substantial increase of the hardness of DLC films as well (see e. g. [2]). However, in [17, 18, 20] hardness of DLC:SiO_x films deposited by ICP PECVD was <16 GPa, despite presence of crystalline SiO_x nanoclusters in [17]. Surprisingly hardness of the diamond like nanocomposite films deposited by using another high plasma density synthesis method (deposition by ECWR plasma beam source) did not exceed 11 GPa [39, 41].

Hardness >15 GPa was reported in [22, 24 – 26] for films deposited by hot filament (electron emission) activated PECVD from different siloxane (vapour) based precursors. However, it should be mentioned, that in [26] >15 GPa hardness was observed for DLC:SiO_x films of chemical composition 18 at.% Si and 7 at.% O and up to 21 GPa hardness for Si and O concentrations less than 5 at.%. Similarly in [21] relatively low Si and O content (C/Si atomic concentration ratio in 0.34 – 0.67 range, O/C in 0.12 – 0.18 range) was reported for DLN films deposited by hot filament activated PECVD. Thus it seems, that in this case rather take place changes in chemical reactions during DLC:SiO_x film growth due to the activation of the siloxane molecules dissociation than increase of the plasma density.

Hardness of the DLC:SiO_x films deposited by a closed drift ion source from HMDSO and hydrogen or HMDSO and He gas mixture was in 6 GPa – 13 GPa range [28], while XPS study revealed relatively large atomic concentrations in such a films (Si atomic concentration in (18 – 20) at.% range, O – in (22 – 27) at% range) [30]. It is similar to the case of the DLN films deposited by CCP PECVD.

Table 3. Hardness and Young's modulus of DLC:SiO_x and DLC films

Ref.	Deposition method	Reagents used for DLC:SiO_x synthesis	Hardness (GPa)		Young's modulus (GPa)		Chemical composition of DLC:SiO_x films (at%)
			DLC:SiO_x	DLC*	DLC:SiO_x	DLC*	
[12]	RF CCP PECVD	HMDSO based	7–10	20-30			30 at.% Si, 23 at.% O
[14]	RF CCP PECVD	HMDSO/Ar	9.8 ±0.7	20±5	88 ±7		
[10]	RF/DC PECVD	HMDSO	12		98		
[9]	RF CCP PECVD	HMDSO	12–13		100		
[8]	RF CCP PECVD	TEOS/CH_4	9–17	20	85–135	170	
[13]	RF CCP PECVD	TEOS/CH_4/Ar	17				57.9 % C, 32.8 % O, 9.3 % Si
[11]	RF CCP PECVD	HMDSO/CH_4/Ar	8–25				
[7]	RF CCP PECVD	HMDSO/CH_4	15–23	24	95–130	159	>39 at.% C, <3 at.% O, <12 at.% Si, >46 at.% H (RBS)
[15]	RF CCP PECVD	CH_4/SiH_4/O_2	10–15				>36 % C, <46 % O, <17 % Si
[16]	Puls. CCP PECVD	TEOS/Ar	9–14	17.5			5–24 at.% Si
[56]	RF CCP PECVD ICP PECVD		5.5–6.9 11.5–13.5		48–63 76–80		
[18]	ICP PECVD	C_2H_2/TMS/O_2	10–12	13.1			Si/C 0.09–0.17, O/C 0.06–0.25
[20]	ICP PECVD	HMDSO/O_2	10–13				
[17]	ICP PECVD	HMDSO	12–16		93–100		
[19]	ICP PECVD	HMDSO	25–30	25–30			
[39, 41]	ECWR plasma beam	HMDSO	6–11		40–80		C/Si 0.34–0.67, O/C 0.12–0.18
[21]	Hot filament PECVD	Siloxane vapor	15 20		130 160		20–35 at.% H, 42–58 at.% C, 15 at.% Si, 7 at.% O (RBS)
[23-24]		Siloxane precursor	8.2–17		90–160		
[25]		Siloxane precursor	12–17		88–128		
[22]		Liquid PPMDSO	15–17				
[26]		Siloxane precursor	12–21				5–36 at.% Si, 5–17 at.% O
[28]	CDIBS	HMDSO/H_2 HMDSO/He	8–12 6–13				

*DLC was deposited at the same technological conditions employing only hydrocarbon gas.

In [26] hardness decreased with increase of the Si and O atomic concentration in film from 17 GPa – 21 GPa for film with <5 % Si and <5 % O to the 12 GPa – 14 GPa in the case of the DLC:SiO$_x$ film of the composition 36 % Si and 17 % O. The drop in hardness was explained by replacement of C–C bond by siloxane bonds [16]. In [16] hardness of the films with Si concentrations >13 at.% did not decrease any further. It was explained by formation of the composite structure – coexistence of SiO$_x$ and SiO$_x$–DLC in films with Si concentrations >13 at.% [16].

In [16] hardness of DLC:SiO$_x$ film decreased from 17.5 GPa to 9 GPa with increase of the Si concentration from 0 % to 17 %. It seems that increase of the Si concentration above 13 at.% resulted in no further reduction of the hardness with decrease of the stress and was explained by formation of the siloxane-bonded DLC networks and SiO$_x$ clusters instead of the siloxane network alone.

Hardness and reduced modulus of DLC:SiO$_x$ films deposited by RF plasma beam decreased nearly twice with decrease of the C/Si ratio from 2.5 to 1.5 [39, 41].

Hardness and elastic modulus of DLC:SiO$_x$ films deposited by ICP PECVD increased with increase of the substrate bias from 100 V to 400 V from 12 GPa to 16 GPa and from 93 GPa to 100 GPa respectively [17]. In [8] mechanical properties of the DLC:SiO$_x$ film deposited from TEOS/CH$_4$ gas mixture non-monotonically depended on bias voltage – the largest hardness and Young's modulus was reported for films deposited at –200 V bias voltage. These results were in good accordance with structural changes of the DLC films such as sp^3/sp^2 bond ratio and hydrogen amount. In [28] hardness of the DLC:SiO$_x$ films deposited from HMDSO/H$_2$ or HMDSO/He gas mixtures non-monotonically depended on ion energy as well. Yet in [15] hardness of DLC:SiO$_x$ films increased from 10 GPa to 15 GPa with increase of the substrate bias from –100 V to –500 V. In [20] hardness of the DLC:SiO$_x$ film deposited by ICP PECVD increased from 10 GPa to 13 GPa with increase of the ICP plasma power from 150 W to 300 W.

Hardness of DLC:SiO$_x$ films non-monotonically depended on HMDSO and CH$_4$ gas flux ratio: the highest hardness of 25 GPa was reported in the case of the flux ratio 0.25, while in the case of the low flux ratio hardness was below 15 GPa and in the case of the high flux rate hardness dropped below 10 GPa [11]. However in [7] hardness of DLC:SiO$_x$ films was lower than hardness of DLC films and decreased with increase of the HMDSO/CH$_4$ ratio, yet decrease of the hardness was relatively small for ratios below 0.3 and hardness of the films was <20 GPa only when HMDSO/CH$_4$ ratio exceeded 0.4. In this case decrease of the Young's modulus was more substantial – modulus of DLC was 160 GPa, while Young's modulus of DLC:SiO$_x$ in all cases was reported to be <130 GPa [7]. It should be mentioned, that in [7] Si concentration was <12 at.% and O concentration was <3 at.% even for HMDSO/CH$_4$ flux ratio 0.6. It should be mentioned, that in [18] hardness of the SiO$_x$ containing DLC film non-monotonically depended on chemical composition of the film as well.

It should be mentioned, that hydrogen content in film has significant influence on hardness of the DLC films [2]. It can be seen in 1 – 5 tables, that various reagents with different hydrogen content were used for synthesis of DLC:SiO$_x$ films. Therefore it can be supposed, that differences in hydrogen content in diamond like nanocomposite films have influence on hardness of DLC:SiO$_x$ layers as well. However, present data on that matter are very fragmented and incomplete (Table 3).

In addition toughness of SiO$_x$ containing DLC films was higher than toughness of the DLC [7, 22], however its dependence of chemical composition of DLC:SiO$_x$ film was non-monotonic [7].

4.2. Coefficient of friction and wear resistance

Coefficient of friction of DLC:SiO$_x$ films in most cases was lower than the friction coefficient of DLC films. Only in [12] friction coefficient of DLC:SiO$_x$ films was reported to be about twice higher than friction coefficient of DLC films. However, in [57] friction coefficient of DLC:SiO$_x$ with steel was about 1.5 – 2 times lower than friction coefficient of DLC film (0.05 – 01 and 0.1 – 0.2 respectively). Friction coefficient of the DLC:SiO$_x$ against WC/Co ball was nearly two times lower than friction coefficient of the DLC [8]. Coefficient of friction of DLC:SiO$_x$ with steel or WC was reported to be in 0.04 – 0.06 range [10, 58]. In [24] friction coefficient in 0.02 – 0.05 range was reported, too.

In [26] coefficient of friction of the DLC:SiO$_x$ non-monotonically depended on chemical composition. The lowest reported friction coefficient was in 0.04 – 0.08 range and the highest – 0.1 – 0.2. Friction coefficient of DLC:SiO$_x$ increased with substrate bias [8] – friction coefficient <0.05 was observed in the case of the films deposited at –100 V and –200 V bias, while friction coefficient increased >2 times with increase of the substrate bias up to –500 V.

Friction coefficient of the SiO$_x$ containing DLC films depended on applied load [23]. At a normal load of 98 mN (contact stress of 514 MPa), friction coefficient of DLC:SiO$_x$ deposited on Ni substrate steady-state value was 0.061 ±0.002, at 490 mN (875 MPa) friction coefficient was 0.094 ±0.014 and in the case of the applied load of 980 mN (1101 MPa), friction coefficient increased up to 0.283 ±0.020 (it is close to the value of the bare Ni). Increase of the friction coefficient with applied load was reported in [25], too.

It must be mentioned, that the coefficient of friction of DLC:SiO$_x$ films, as measured in air of 50 % relative humidity (RH) using steel counter body was in 0.04 – 0.08 range and even in humid air of 90 % RH and under water, the coefficient of friction was <0.1 [22]. In [8] friction coefficient of DLC:SiO$_x$ measured under water was slightly higher than friction coefficient measured in air 30 % – 40 % RH– no sudden increase of friction coefficient typical for DLC was observed.

Low friction coefficient of DLC:SiO$_x$ films was explained by low surface energy of the DLC:SiO$_x$, implying weak interaction and mutual bonding [57]. However, in [12] friction coefficient of DLC:SiO$_x$ films was higher than friction of DLC film despite low surface energy. In [59] low friction of SiO$_x$ containing DLC films was explained by the interfacial sliding between the DLC:SiO$_x$ film and the friction-induced transfer film adhered to the friction (wear) test ball counterface. The transfer films generated in humid air were enriched with SiO_2 containing fragments, whereas transfer films formed in dry nitrogen had hydrogenated and long range ordered carbons with practically no SiO_2 fragments [59].

Wear resistance of DLC:SiO_x was 15 – 20 times lower in comparison with DLC film deposited from CH_4 gas [12]. Similarly wear rate against steel was substantially higher in the case of DLC:SiO_x film in comparison with DLC film despite lower friction coefficient of DLC:SiO_x [57]. In [26] wear resistance of the DLC:SiO_x films decreased with increased concentration of Si and O. It rather correlated with decreased nanohardness of the films even despite decreased friction coefficient. In [17] wear resistance of the ICP PECVD deposited DLC:SiO_x films increased with substrate bias in –100 V – –400 V range. In this case wear resistance increased with hardness of the films. It should be mentioned, that differently from DLC films, DLC:SiO_x films have high wear resistance to the wear in water [22]. It correlates with relatively low friction coefficient of DLC:SiO_x in water [22].

In general, DLC doping with SiO_x results in a substantial reduction of the residual stress, lower friction coefficient in dry and moderatively humid atmospheres. In such a way substantially thicker films with increased fracture toughness can be synthesized. However, deposition conditions of the DLC:SiO_x film must be carefully selected to fabricate films with hardness, Young's modulus and wear resistance in air close to those of DLC film. In such a case along with the ion energy it is very important to achieve high plasma density. Structure and, especially, chemical composition of the films must be carefully optimized as well, because optimum ion energy and high plasma density alone do not ensure fabrication of the DLC:SiO_x films with high hardness (>20 GPa). Therefore, application of the multilayer DLC:SiO_x/DLC films can be advantageous as it was suggested e. g. in [60].

5. OPTICAL PROPERTIES

Evaluation of amorphous semiconductors requires parameterization of the photon energy dependence of the optical constants (refractive index, extinction coefficient) [61]. Hydrogenated amorphous carbon (a-C:H) involves coexistence of sp^2 and sp^3 hybridized carbon sites, hence it has both σ and π electrons. The optical properties of amorphous C films are known to be dominated by π-π^* and σ-σ^* electronic transitions, along with π-σ^* and σ-π^* transitions [2,62]. Optical absorption measurements are widely used to characterize the electronic properties of materials, through the determination of parameters describing the electronic transitions such as: band gap, valence band tails and lifetime of excited state, which can be related to disorder in the material network, i. e. bond strength and defects. Several models are commonly used to determine the optical properties of amorphous semiconductors and dielectrics in the energy range of interband transitions [61]. Such parameters as optical band gap E_g (Tauc gap), energy E_{04}, and Urbach energy E_U are used to describe properties of amorphous carbon.

The incorporation of silicon and oxygen impurities in the DLC films causes change in their optical properties (optical band gap, refractive index). Increase of the optical bandgap as well as shift of absorbance edge and drastic increase of transparency of the films was reported (see Fig. 3) [18, 29, 63, 64].

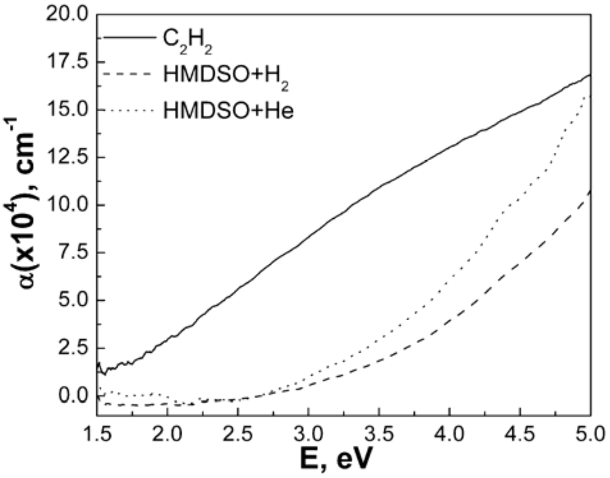

Fig. 3. Absorption coefficient dependence on the photon energy of films made from different precursors employing CDIBS (500 eV ion beam energy)

Table 4. Optical properties of SiO_x incorporated DLC films

Deposition method and precursor	E_{opt}, eV		n		Ref.
	DLC:SiO_x	DLC	DLC:SiO_x	DLC	
ICP-CVD; C_2H_2/TMS/O_2	2.08–2.32	1.78	1.62–1.72	1.84	[18]
DC PECVD; TEOS/Ar	1.1–3.3	–	–	–	[16]
PECVD; CH_4/SiH_4/O_2	–	1–1.3	1.62–1.7	–	[15, 64]
RF PECVD; CH_4/SiH_4/O_2	1.8–3	–	–	–	[43]
RF PECVD; CH_4/HMDSO	–	–	2–2.1	1.97	[7]
CDIBS; HMDSO/H_2	2.09–2.74	0.8–1.7	1.85–1.98	2.53–2.71	[29, 63]
CDIBS; HMDSO/He	2.19–2.45	–	1.85–2.01	–	[29]
CDIBS; HMDSO/H_2	3.12	–	1.7	–	[36]
CDIBS; HMDSO/C_2H_2	1.6	–	2.1	2.2–2.3	[36]
CDIBS; HMDSO/H_2	3.12	–	1.8	–	[30]
CDIBS; HMDSO/H_2/Ar	3.21	–	1.8	–	[30]
CDIBS; HMDSO/H_2/N_2	3.51–3.58	–	1.7–1.8	–	[30]
CDIBS; HMDSO	–	–	2.1–2.5	–	[37]
CDIBS; HMDSO	1.45–2.44	–	–	–	[35]

Optical band gap of DLC:SiO_x films can be changed in a wide region from 1.1 eV to 3.3 eV, while refractive index was reported to be in 1.62 – 2.5 range (see Table 4). The band gap and refractive index of DLC:SiO_x films depends on the deposition energy and precursor/carrier gas used during process. The decrease of refractive index with increase of ion beam energy was observed, while optical band gap showed non monotonous dependence on the ion beam energy [29].

It was reported that optical band gap increases with the increase of oxygen and silicon content in the films. This is due to incorporation of Si–O bonds in the DLC films, since SiO_x network has wider band gap compared to Si-C_x network [18]. Similarly to the dependence of the hardness on the silicon content, the band gap of the films is also dependent on the silicon content in the films. In [16] it was observed that at low Si concentrations the band gap is around 1.1 eV – 1.5 eV, and only when Si content exceeds 13 at.%, the band gap increases to 3.3 eV. The increase of optical band gap of DLC films with incorporated separately oxygen or silicon was also observed but it was much lower compared to DLC:SiO_x [43]. These results confirm that optical band gap in DLC:SiO_x films is governed by existence of segregated phases of SiO_x-DLC and SiO_x in the films [16]. The refractive index of DLC:SiO_x films might be as low as 1.62 [15, 18, 64], because softer and less-stressed a-SiO_x network reduces density of the DLC:SiO_x films [18]. The band gap and refractive index of the films strongly depends on the deposition conditions of DLC:SiO_x. In [15] the influence of the bias voltage was determined. It was observed that refractive index increases and band gap decreases with increase of self-bias voltage. The observed increase of the refractive index is related to the increased carbon density of the amorphous network which shortens the optical gap as bias voltage is increased [15]. Two effects contributing to the reduction of the optical gap and increase of refractive index may take place when bias voltage is increased to more negative values: 1) a relative change from SiO_x rich phase to a DLC-rich one; 2) an increase of sp^2 character of carbon bonds, in a similar way to what occurs in case of DLC films [15].

6. ELECTRICAL AND DIELECTRIC PROPERTIES. THERMAL CONDUCTIVITY

In several studies DLC:SiO_x films were investigated as a potential low dielectric constant insulator. Dielectric permittivity of DLC:SiO_x films deposited by CDIBS is in 3 – 3.8 range [31, 34] – that is lower than dielectric permittivity value of SiO_2 (3.9 – 4.2 [65]). Dielectric breakdown strength routinely was in (1 – 2) MV/cm range [31, 34, 66]. It depended on substrate used for deposition of DLC:SiO_x film (Ti, Si, Al, Cr) [35]. Such dependence was described by different structure of the films as well as different roughness of the used substrates [34]. It should be mentioned, that in [66] for some DLC:SiO_x coatings breakdown strength as high as 500 MV/cm was reported.

The main charge transfer mechanisms of DLC:SiO_x film was reported to be space charge limited current with exponential or Gaussian trap distribution [67] and Poole- Frenkel emission in [34].

Thermal conductivity of DLC:SiO_x films was 0.76 W/cmK) [68]. It is slightly higher than thermal conductivity of the hydrogenated DLC films – (0.56 – 0.69) W/cmK [69], (0.3 – 0.5) W/cmK [70]. However, thermal conductivity of the DLC:SiO_x films is lower than thermal conductivity of the hydrogenated tetrahedral amorphous carbon and tetrahedral amorphous carbon (sp^3 bonded carbon amount ≥70 %) ((0.77 – 1.3) W/cmK and (1.41 – 5) W/cmK respectively [69, 71]) as well as thermal conductivity of the silicon dioxide ((1 – 1.5) W/cmK [71]).

7. SURFACE FREE ENERGY AND CONTACT ANGLE WITH WATER

Surface free energy (contact angle with water) of DLC:SiO_x films is reported to be in relatively wide range depending on the deposition conditions as well as chemical composition of the synthesized film. It can be seen in Fig. 4 and Table 5, that minimum contact angle with water values reported by different authors was slightly below value typical for undoped hydrogenated DLC films (56°) [15], while maximum reported contact angle of DLC:SiO_x film was close to the contact angle of such a highly hydrophobic film as Teflon (PTFE) (100°) [12, 14]. These highly hydrophobic DLC:SiO_x films were moderate hard (7 GPa – 10 GPa) [12, 14]. By combining nano-scale surface roughening with a hydrophobic a-C:H:Si:O coating, the super-hydrophobic surface with a wetting angle around 160° was fabricated [72]. For DLC:SiO_x films deposited by pulsed CCP PECVD from TEOS, the dispersive surface energy component decreased (increased contact angle with water) when Si concentration was (9 – 14) at.%, while slight increase was observed for Si concentrations below 9 at.% [46]. However in [37] contact angle decreased with the increase of the silicon concentration up to (20 – 23) at.% range. Wetting angle of DLC:SiO_x film deposited by RF PECVD from $CH_4/SiH_4/O_2$ gas mixture decreased from 72° to 64° with increase of the oxygen concentration in plasma from 0 % to 5 % [43]. However, it should be mentioned, that even in the case of the film deposited from CH_4/SiH_4 gas mixture atomic oxygen concentration in synthesized DLC film was about two times higher than concentration of the silicon (~16 at.% and ~8 at.% respectively).

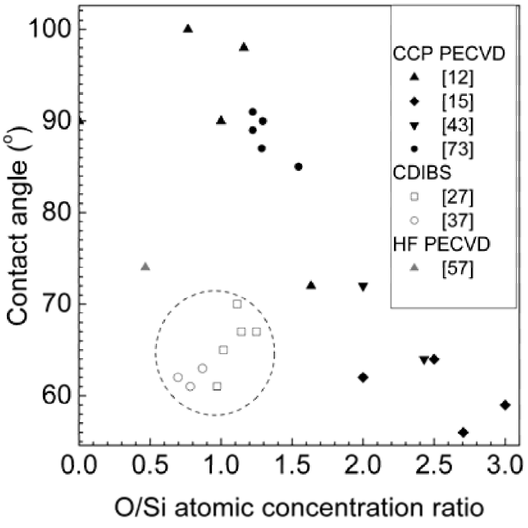

Fig. 4. The dependence of the contact angle with water of DLC:SiO_x films on O/Si atomic concentration ratio. O/Si = 0 point refer to Si containing DLC film

No dependence of the contact angle of the DLC:SiO_x film deposited by a CDIBS from HMDSO vapour on O concentration at constant atomic concentration of the Si was observed in [37]. In [12] there was reported, that addition of oxygen to the Si containing DLC film reduces surface free energy, as long as the O concentration in the coating is kept below a critical concentration of approximately 35 at.% when Si atomic concentration is ~30 at.%. With such O incorporation the dispersive component can be reduced significantly from 31 mN/m to 23.5 mN/m. The reduction of the dispersive component is correlated with a slight increase of the polar component (2.0 mN/m to 3.7 mN/m), because oxygen is partly incorporated into the network, with a polar binding type like Si-OH [12]. For O concentrations >35 at.%, a significant increase of the surface free energy as a result of the increase of the polar component was reported [12]. Similarly in [37] non-monotonic dependence of the contact angle on O/Si atomic concentration ratio was observed with maximum contact angle at O/Si ratio ~1.1.

Table 5. Surface free energy, contact angle with water and chemical composition of DLC:SiO_x films

Deposition method and precursor	Surface energy (mN/m)	Contact angle with water, °	Chemical composition (at, %)			Ref.
			C	O	Si	
CCP PECVD HMDSO	18.4	~110	PTFE			[12]
	24	100	–	23	30	
	–	~72	–	49	30	
	31	90	70	0	30	
	23.5	90	40	30	30	
CCP PECVD HMDSO/Ar	22.9	101	–	–	–	[14]
CCP PECVD $CH_4/SiH_4/O_2$	–	64	52	34	14	[43]
	–	72	76	16	8	
CCP PECVD $CH_4/SiH_4/O_2$	–	56	37	46	17	[15]
	–	64	51	35	14	
	–	62	65	24	12	
	–	59	68	24	8	
CCP PECVD HMDSO/Ar	–	101.8	–	–	–	[72]
CCP PECVD TEOS	–	89	60	22	18	[73]
	–	91	60	22	18	
	–	90	61	22	17	
TEOS/Ar	–	87	68	18	14	
	–	85	72	17	11	
	–	89	60	22	18	
CDIBS $HMDSO/H_2$	–	67	55.32	23.83	20.85	[27]
	–	67	51.34	27.02	21.64	
	–	70	57.2	22.55	20.25	
	–	65	56.12	22.12	21.75	
	–	61	55.9	21.74	22.36	
	–	67	55.32	23.83	20.85	
CDIBS HMDSO	–	63	57	20	23	[37]
	–	61	59	18	23	
	–	62	61	16	23	

It seems, that surface free energy of the films deposited from organosilicon vapour (HMDSO) is lower in comparison with surface energy of the film deposited from the mixture of TMS/O_2 [12].

Some dependence of contact angle on ion energy used for deposition of the film was reported in [15]. Weak dependence of contact angle on deposition energy (bias voltage) was observed – the highest contact angle was observed in the case of the film with the highest sp^3/sp^2 ratio (highest stress level).

It seems, that different studies present rather controversial data about the dependence of the contact angle with water on chemical composition of DLC:SiO_x films. Complex analysis of the all reported data revealed no clear dependence of the contact angle on Si, O or C atomic concentration alone. The contact angle vs O/Si atomic concentration ratio is presented in Fig. 4. It can be seen, that according to Fig. 4 and [12] for DLC:SiO_x films deposited by CCP PECVD the highest contact angle with water (~100°) is observed when O/Si ratio is close to 1. Further increase of the O/Si ratio results in nearly linear decrease of the hydrophobicity of the film. In the case of the DLC:SiO_x films deposited by closed drift ion beam source, increase of the O/Si atomic concentration ratio up to ~1.1 resulted in increase of the contact angle. It seems that in this case some small peak of the hydrophobicity at O/Si ratio ~1.1 can be observed. The observed results are in good accordance with explanation suggested in [46], that changes of the surface energy of DLC:SiO_x films are related to transition of the chemical structure of the film from siloxane (O/Si ratio ~1) to silsesquioxane (O/Si ratio ~1.5) [16, 46] as well as formation of the SiO_x phase [16]. Differences between the contact angle of the DLC:SiO_x films deposited by CCP PECVD and CDIBS probably can be explained by higher ion energy during deposition in the case of the ion beam synthesis, because CDIBS usually operates in >300 eV ion beam energies range [28] what is substantially more than 100 eV energy optimum for deposition of the DLC films [2].

8. APPLICATIONS

Diamond like nanocomposite (DLC:SiO_x) films are commercialized under the tradename DYLYN by Belgium based Bekaert company. Current applications of the DYLYN and DYLYN/DLC films include reduction of the friction and wear in car engines, plastic mould components, optical disc mould parts, textile machinery.

DLC:SiO_x can be used in MEMS technology both as a surface coating material or a structural material. In [24], use of DLN films as a coating material for decrease of the wear and friction of micro components as well as reduction of the sticking between microstructure and the substrate was suggested. SiO_x containing diamond like carbon film was applied as an effective barrier for protection of the microstructures against stiction during fabrication of surface micromachined electrostatically actuated microelectromechanical switch [74]. Application of the DLC:SiO_x as a structural material for MEMS fabrication was reported in [32] – DLC:SiO_x based free-standing cantilevers and bridges were fabricated.

There were suggested to use DLC:SiO_x film as an antireflective coating of the crystalline Si solar cell [63].

SiO_x containing DLC films were applied as an imprint stamp antisticking layers in nanoimprint lithography [30, 75]. The feasibility of applying DLN coatings on the sidewalls of LIGA (lithography, electroplating, and moulding) fabricated microsystem parts by commercial PECVD techniques has been demonstrated in [76]. In such a way problems related with handling of the miniature LIGA parts during deposition were solved.

Cell adhesion, cytotoxicity and macrophage adhesion tests revealed good biocompatibility of the diamond like nanocomposite films [77]. Covering of the stent by DLC:SiO_x resulted in decreased thrombogenicity and decreased neointimal hyperplasia [78]. While deposition of the additional DLC films resulted in increased inflammatory reaction [78].

CONCLUSIONS

DLC:SiO_x (diamond like nanocomposite) films are a class of the DLC based composite materials which can consist of the interpenetrating networks of a-C:H and SiO_x or SiO_x clusters embedded into the a-C:H matrix. Silicon and oxygen atomic concentration in such films can vary from several percents up to 30 – 40 percents. DLC:SiO_x films can be deposited by different PECVD and ion beam deposition techniques. Internal stress in DLC:SiO_x films is substantially lower than in DLC films, therefore fabrication of the films of thickness of up to 10 micrometers is possible. Toughness of DLC:SiO_x films is higher than toughness of the hydrogenated DLC films as well. However, in most cases it can be achieved at the cost of the decreased hardness and Young's modulus. Hardness and Young's modulus of DLC:SiO_x can be increased by setting appropriate deposition conditions (ion energy, plasma density) as well as by choosing correct structure and chemical composition. In most cases friction coefficient of the DLC:SiO_x films is substantially lower than friction coefficient of the hydrogenated DLC films. However, lower friction coefficient alone did not ensure increase of the wear resistance. It seems, that wear resistance of DLC and DLC:SiO_x films correlates rather with hardness than with the friction coefficient. It should be mentioned, that friction coefficient of DLC:SiO_x remains low in water as well. It is different behaviour in comparison with DLC films. In such a way resistance to the wear in water of DLC:SiO_x is substantially higher than wear resistance of DLC. Mechanical properties mentioned above along with the low refractive index and higher transparency compared with the DLC films makes DLC:SiO_x an attractive choice as a protective films for different optical applications. Contact angle with water of DLC:SiO_x films can be changed in wide range 56° – 100°. Present industrial applications of the DLC:SiO_x films include low friction wear resistant coatings for increased lifetime of the car engines, plastic mould components, optical disc mould parts, textile machinery parts. Use of these films for different lithography techniques, MEMS fabrication as well as in biomedicine is considered.

Acknowledgments

The article was prepared under support of the European Social Fund Agency implementing measure VP1-3.1-ŠMM-05-K of the Human Resources Development Operational Programme of Lithuania 2007-2013 3rd priority "Strengthening of capacities of researchers and scientists" (project No. VP1-3.1-ŠMM-05-K-01-003).

REFERENCES

1. **Aisenberg, S., Chabot, R.,** Deposition of Carbon Films with Diamond Properties *Carbon* 10 1972: p. 356.
2. **Robertson, J.,** Diamond-like Amorphous Carbon *Materials Science and Engineering R* 37 2002: pp. 129 – 281.
3. **Casiraghi, C., Robertson, J., Ferrari, A. C.** Diamond-like Carbon for Data and Beer Storage *Materials Today* 10 2007: pp. 44 – 53.
4. **Luo, J. K., Fu, Y. Q., Le, H. R., Williams, J. A., Spearing, S. M., Milne, W. I.** Applications of Diamond and Diamond-like Carbon in MEMS *Journal of Micromechanics and Microengineering* 17 2007: pp. S147 – S163. http://dx.doi.org/10.1088/0960-1317/17/7/S12
5. **Robertson, J.** Comparison of Diamond-like Carbon to Diamond for Applications *Physica Status Solidi A* 205 2008: pp. 2233 – 2244.
6. **Dorfman, V. F.** Diamond-Like Nanocomposites (DLN) *Thin Solid Films* 212 1992: p. 267. http://dx.doi.org/10.1016/0040-6090(92)90532-G
7. **Zajickova, L., Bursikova, V., Perina, V., Mackova, A., Janca, J.** Correlation between SiO_x Content and Properties of DLC:SiO_x Films Prepared by PECVD *Surface and Coatings Technology* 174 – 175 2003: pp. 281 – 285.
8. **Yang, W. J., Sekino, T., Shim, K. B., Niihara, K., Auh, K. H.** Microstructure and Tribological Properties of SiOx/DLC Films Grown by PECVD *Surface & Coatings Technology* 194 2005: pp. 128 – 135.
9. **Santra, T. S., Liu, C. H., Bhattacharyya, T. K., Patel, P., Barik, T. K.** Characterization of Diamond-like Nanocomposite Thin Films Grown by Plasma Enhanced Chemical Vapor Deposition *Journal of Applied Physics* 107 2010: p. 124320.
10. **Santra, T. S., Bhattacharyya, T. K., Patel, P., Tseng, F. G., Barik, T. K.** Structural and Tribological Properties of Diamond-like Nanocomposite Thin Films *Surface & Coatings Technology* 206 2011: pp. 228 – 233. http://dx.doi.org/10.1016/j.surfcoat.2011.06.057
11. **Buršíková, V., Navrátil, V., Zajíčková, L., Janča, J.** Temperature Dependence of Mechanical Properties of DLC/Si Protective Coatings Prepared by PECVD *Materials Science and Engineering A* 324 2002: pp. 251 – 254. http://dx.doi.org/10.1016/S0921-5093(01)01320-X
12. **Grischke, M., Hieke, A., Morgenweck, F., Dimigen, H.** Variation of the Wettability of DLC-coatings by Network Modification Using Silicon and Oxygen *Diamond and Related Materials* 7 1998: pp. 454 – 458.
13. **Yang, W. J., Niihara, K., Auh, K. H.** Structural Modifications of SiO_x/DLC Films by Thermal Annealing *Journal of Ceramic Processing Research* 5 2004: pp. 269 – 273.
14. **Schiffmann, K. I., Hieke, A.** Analysis of Microwear Experiments on Thin DLC Coatings: Friction, Wear and Plastic Deformation *Wear* 254 2003: pp. 565 – 572.
15. **Damasceno, J. C., Camargo Jr., S. S.** Plasma Deposition and Characterization of Silicon Oxide-containing Diamond-like Carbon Films Obtained from CH_4:SiH_4:O_2 Gas Mixtures *Thin Solid Films* 516 2008: pp. 1890 – 1897. http://dx.doi.org/10.1016/j.tsf.2007.10.119

16. **Randeniya, L. K., Bendavid, A., Martin, P. J., Amin, M. S., Preston, E. W.** Molecular Structure of SiO_x-incorporated Diamond-like Carbon Films; Evidence for Phase Segregation *Diamond & Related Materials* 18 2009: pp. 1167 – 1173. http://dx.doi.org/10.1016/j.diamond.2009.03.004
17. **Chen, L.-Y., Hong, F. C.-N.** Effects of SiO_x-incorporation Hydrocarbons on the Tribological Properties of DLC Films *Diamond & Related Materials* 10 2001: pp. 1058 – 1062. http://dx.doi.org/10.1016/S0925-9635(00)00573-2
18. **Baek, S.-M., Shirafuji, T., Saito, N., Takai, O.** Adhesion Property of SiO_x-doped Diamond-like Carbon Films Deposited on Polycarbonate by Inductively Coupled Plasma Chemical Vapor Deposition *Thin Solid Films* 519 2011: pp. 6678 – 6682.
19. **Chen, L.-Y., Hong, F. C.-N.** Diamond-like Carbon Nanocomposite Films *Applied Physics Letters* 82 2003: pp. 3526 – 3528. http://dx.doi.org/10.1063/1.1576909
20. **Guo, Y.-B., Hong, F. C.-N.** Adhesion Improvements for Diamond-like Carbon Films on Polycarbonate and Polymethylmethacrylate Substrates by Ion Plating with Inductively Coupled Plasma *Diamond and Related Materials* 12 2003: pp. 946 – 952.
21. **Zsidai, L., Samyn, P., Vercammen, K., Van Acker, K., Kozma, M., Kalácska, G., De Baets, P.** Friction and Thermal Effects of Engineering Plastics Sliding against Steel and DLN-coated Counterfaces *Tribology Letters* 17 2004: pp. 269 – 288. http://dx.doi.org/10.1023/B:TRIL.0000032453.09366.d4
22. **Neerinck, D., Persoone, P., Sercu, M., Goel, A., Venkatraman, C., Kester, D., Halter, C., Swab, P., Bray, D.** Diamond-like Nanocomposite Coatings for Low-wear and Low-friction Applications in Humid Environments *Thin Solid Films* 317 1998: pp. 402 – 404. http://dx.doi.org/10.1016/S0040-6090(97)00631-7
23. **Jungk, J. M., Michael, J. R., Prasad, S. V.** The Role of Substrate Plasticity on the Tribological Behavior of Diamond-like Nanocomposite Coatings *Acta Materialia* , 56 2008: pp. 1956 – 1966. http://dx.doi.org/10.1016/j.actamat.2007.12.048
24. **Santra, T. S., Bhattacharyya, T. K., Tseng, F. G., Barik, T. K.** Diamond-Like Nanocomposite (DLN) Films for Microelectro-Mechanical System (MEMS) *Proceedings Published by International Journal of Computer Applications* 2011: pp. 6 – 9.
25. **Scharf, T. W., Singer, I. L.** Monitoring Transfer Films and Friction Instabilities with in Situ Raman Tribometry *Tribology Letters* 14 2003: pp.3 – 8. http://dx.doi.org/10.1023/A:1021942830132
26. **Neerinck, D., Persoone, P., Sercu, M., Goel, A., Kester, D., Bray, D.** Diamond-like Nanocomposite Coatings (a-C:H/a-Si:O) for Tribological Applications *Diamond and Related Materials* 7 1998: pp. 468 – 471. http://dx.doi.org/10.1016/S0925-9635(97)00201-X
27. **Meškinis, Š., Tamulevičius, S., Kopustinskas, V., Andrulevičius, M., Guobienė, A., Gudaitis, R., Liutvinienė, I.** Hydrophobic Properties of the Ion Beam Deposited DLC Films Containing SiO_x *Thin Solid Films* 515 2007: pp. 7615 – 7618. http://dx.doi.org/10.1016/j.tsf.2006.11.089
28. **Tamulevičienė, A., Meškinis, Š., Kopustinskas, V., Tamulevičius, S.** Carrier Gas and Ion Beam Parameter Effects on the Structure and Properties of a-C:H/SiO_x Films Deposited Employing Closed Drift Ion Beam Source *Nuclear Instruments and Methods in Physics Research Section B* 2011. doi:10.1016/j.nimb.2011.08.064.
29. **Tamulevičienė, A., Kopustinskas, V., Meškinis, Š., Tamulevičius, S.** Deposition of SiO_x Containing DLC Films Using Different Transport Gas in a Closed Drift Ion Beam Source *Program and Materials of 3rd International Conference "Radiation Interaction with Materials and Its Use in Technologies"* Kaunas, Lithuania, 2010: pp. 169 – 172.
30. **Meškinis, Š., Kopustinskas, V., Šlapikas, K., Tamulevičius, S., Guobienė, A., Gudaitis, R., Grigaliūnas, V.** Ion Beam Synthesis of the Diamond-like Carbon Films for Nanoimprint Lithography Applications *Thin Solid Films* 515 2006: pp. 636 – 639. http://dx.doi.org/10.1016/j.tsf.2005.12.223
31. **Meškinis, Š., Gudaitis, R., Tamulevičius, S., Kopustinskas, V., Andrulevičius, M.,** Dielectric Properties of the Ion Beam Deposited SiO_x Doped DLC Films, *Materials Science* (*Medžiagotyra*) 15 2009: pp. 3 – 6.
32. **Meškinis, Š., Tamulevičius, S., Kopustinskas, V., Gudonytė, A., Grigaliūnas, V., Jankauskas, J., Gudaitis, R.** Micromachining of Diamond-like Carbon Deposited by Closed Drift Ion Source for Cantilevers and Membranes *Materials Science* (*Medžiagotyra*) 15 2009: pp. 201 – 206.
33. **Meškinis, Š., Kopustinskas, V., Tamulevičiene, A., Tamulevičius, S., Niaura, G., Jankauskas, J., Gudaitis, R.** Ion Beam Energy Effects on Structure and Properties of Diamond-like Carbon Films Deposited by Closed Drift Ion Source *Vacuum* 84 2010: pp. 1133 – 1137. http://dx.doi.org/10.1016/j.vacuum.2010.01.047
34. **Meškinis, Š., Šlapikas, K., Gudaitis, R., Tamulevičius, S., Kopustinskas, V., Guobienė, A., Niaura, G.** SiO_x-doped DLC Films: Charge Transport, Dielectric Properties and Structure *Vacuum* 82 2008: pp. 617 – 622. http://dx.doi.org/10.1016/j.vacuum.2007.09.007
35. **Meškinis, Š., Andrulevičius, M., Šlapikas, K., Iljinas, A., Gudaitis, R., Puišo, J., Tamulevičius, S.** Growth and Properties of the Ion Beam Deposited SiO_x Containing DLC Films *Vacuum* 83 2009: pp. S121 – S123.
36. **Kopustinskas, V., Meškinis, Š., Tamulevičius, S., Andrulevičius, M., Čižiūtė, B., Niaura, G.** Synthesis of the Silicon and Silicon Oxide Doped a-C:H Films from Hexamethyldisiloxane Vapor by DC Ion Beam *Surface & Coatings Technology* 200 2006: pp. 6240 – 6244.
37. **Meškinis, Š., Gudaitis, R., Šlapikas, K., Tamulevičius, S., Andrulevičius, M., Guobienė, A., Puišo, J., Niaura, G.** Ion Beam Energy Effects on Structure and Properties of SiO_x Doped Diamond-like Carbon Films *Surface and Coatings Technology* 202 2008: pp. 2328 – 2331. http://dx.doi.org/10.1016/j.surfcoat.2007.08.035
38. **Scharf, T. W., Singer, I. L.** Thickness of Diamond-like Carbon Coatings Quantified with Raman Spectroscopy *Thin Solid Films* 440 2003: pp. 138 – 144.
39. **Tóth, A., Mohai, M., Ujvári, T., Bertóti, I.** Nanomechanical Properties of Silicon-, Oxygen- and Nitrogen-containing a-C:H Films Prepared by RF Plasma Beam CVD *Thin Solid Films* 482 2005: pp. 188 – 191. http://dx.doi.org/10.1016/j.tsf.2004.11.168
40. **Veres, M., Koos, M., Toth, S., Fule, M., Pocsik, I., Toth, A., Mohai, M., Bertoti, I.** Characterization of a-C:H and Oxygen Containing Si:C:H Films by Raman Spectroscopy and XPS *Diamond & Related Materials* 14 2005: pp. 1051 – 1056.

41. **Tóth, A., Mohai, M., Ujvári, T., Bertóti, I.** Surface and Nanomechanical Properties of Si:C:H Films Prepared by RF Plasma Beam CVD *Diamond & Related Materials* 14 2005: pp. 954 – 958.

42. **Ding, X.-Z., Zhang, F.-M., Liu, X.-H., Wang, P. W., Durrer, W. G., Cheung, W. Y., Wang, S. P., Wilson, I. H.** Ion Beam Assisted Deposition of Diamond-like Nanocomposite Films in an Acetylene Atmosphere *Thin Solid Films* 346 1999: pp. 82 – 85.

43. **Damasceno, J. C., Camargo Jr., S. S.** DLC-SiO_x Nanocomposite Films Deposited from CH_4 :SiH_4 :O_2 Gas Mixtures *Surface & Coatings Technology* 200 2006: pp. 6279 – 6282.

44. **Bursikova, V., Sladek, P., St'ahel, P., Zajickova, L.** Improvement of the Effiency of the Silicon Solar Cells by Silicon Incorporated Diamond-like Carbon Antireflective Coatings *Journal of Non-Crystalline Solids* 299 – 302 2002: pp. 1147 – 1151.

45. **Franta, D., Ohlidal, I., Bursikova, V., Zajickova, L.** Optical Properties of Diamond-like Carbon Films Containing SiO_x *Diamond and Related Materials* 12 2003: pp. 1532 – 1538. http://dx.doi.org/10.1016/S0925-9635(03)00221-8

46. **Randeniya, L. K., Bendavid, A., Martin, P. J., Amin, Md. S., Preston, E. W., Magdon Ismail, F. S., Coe, S.** Incorporation of Si and SiO_x into Diamond-like Carbon Films: Impact on Surface Properties and Osteoblast Adhesion *Acta Biomaterialia* 5 2009, , pp. 1791 – 1797.

47. **Yang, W. J., Choa, Y.-H., Sekino, T., Shim, K. B., Niihara, K., Auh, K. H.** Structural Characteristics of Diamond-like Nanocomposite Films Grown by PECVD *Materials Letters* 57 2003: pp. 3305 – 3310. http://dx.doi.org/10.1016/S0167-577X(03)00053-3

48. **Park, C. K., Chang, S. M., Uhm, H. S., Seo, S. H., Park, J. S.** XPS and XRR Studies on Microstructures and Interfaces of DLC Films Deposited by FCVA Method *Thin Solid Films* 420 – 421 2002: pp. 235 – 240.

49. **Paik, N.** Raman and XPS Studies of DLC Films Prepared by a Magnetron Sputter-type Negative Ion Source *Surface & Coatings Technology* 200 2005: pp. 2170 – 2174. http://dx.doi.org/10.1016/j.surfcoat.2004.08.073

50. **O'Hare, L.-A., Parbhoo, B., Leadley, S. R.** Development of a Methodology for XPS Curve-fitting of the Si 2p Core Level of Siloxane Materials *Surface and Interface Analysis* 36 2004: pp. 1427 – 1434.

51. **Alexander, M. R., Short, R. D., Jones, F. R., Michaeli, W., Blomfield, C. J.** A Study of HMDSO/O_2 Plasma Deposits Using a High-sensitivity and Energy Resolution XPS Instrument: Curve Fitting of the Si 2p Core Level *Applied Surface Science* 137 1999: pp. 179 – 183. http://dx.doi.org/10.1016/S0169-4332(98)00479-6

52. **Paul, R., Dalui, S., Das, S.N., Bhar, R., Pal, A. K.** Hydrophobicity in DLC Films Prepared by Electrodeposition Technique *Applied Surface Science* 255 2008: pp. 1705 – 1711.

53. **Li, H., Xu, T., Chen, J., Zhou, H., Liu, H.,** Preparation and Characterization of Hydrogenated Diamond-like Carbon Filmsin a Dual DC-RF Plasma System *Journal of Physics D: Applied Physics* 36 2003: pp.3183 – 3190. http://dx.doi.org/10.1088/0022-3727/36/24/014

54. **Ferrari, A. C., Robertson, J.** Raman Spectroscopy of Amorphous, Nanostructures, Diamond-like Carbon, and Nanodiamond *Philosophical Transactions of the Royal Society A* 362 2004: pp. 2477 – 2512.

55. **Meškinis, Š., Kopustinskas, V., Šlapikas, K., Gudaitis, R., Tamulevičius, S., Niaura, G., Rinnerbauer, V., Hingerl, K.** Optical Properties of the Undoped and SiO_x Doped DLC Films *SPIE Proceedings* 6596 2007: p. 5961L.

56. **Yang, W. J., Choa, Y. H., Sekino, T., Shim, K. B., Niihara, K., Auh, K. H.** Thermal Stability Evaluation of Diamond-like Nanocomposite Coatings *Thin Solid Films* 434 2003: pp. 49 – 54.

57. **Samyn, P., Schoukens, G., Quintelier, J., De Baets, P.** Friction, Wear and Material Transfer of Sintered Polyimides Sliding against Various Steel and Diamond-like Carbon Coated Surfaces *Tribology International* 39 2006: pp. 575 – 589.

58. **Kester, D. J., Brodbeck, C. L., Singer, I. L., Kyriakopoulos, A.** Sliding Wear Behavior of Diamond-like Nanocomposite Coatings *Surface and Coatings Technology* 113 1999: pp. 268 – 273.

59. **Scharf, T. W., Ohlhausen, J. A., Tallant, D. R., Prasad, S. V.** Mechanisms of Friction in Diamond-like Nanocomposite Coatings *Journal of Applied Physics* 101 2007: pp. 063521 (11 p.).

60. **Dekempeneer, E., Van Acker, K., Vercammen, K., Meneve, J., Neerinck, D., Eufinger, S., Pappaert, W., Sercu, M., Smeets, J.** Abrasion Resistant Low Friction Diamond-like Multilayers *Surface and Coatings Technology* 142 – 144 2001: pp. 669 – 673.

61. **Laidani, N., Bartali, R., Gottardi, G., Anderle, M., Cheyssac, P.** Optical Absorption Parameters of Amorphous Carbon Films from Forouhi–Bloomer and Tauc–Lorentz Models: a Comparative Study *Journal of Physics: Condensed Matter* 20 2008: pp. 015216 (8 p.).

62. **Logothetidis, S.** Optical and Electronic Properties of Amorphous Carbon Materials *Diamond & Related Materials* 12 2003: pp. 141 – 150. http://dx.doi.org/10.1016/S0925-9635(03)00015-3

63. **Tamulevičienė, A., Meškinis, Š., Kopustinskas, V., Tamulevičius, S.** Diamond-like Carbon Film as Antireflective Coating for Solar Cells *Materials Science* (*Medžiagotyra*) 16 2010: pp. 103 – 107.

64. **Tamulevičienė, A., Meškinis, Š., Kopustinskas, V., Tamulevičius, S.** Optical Properties of Diamond-like Carbon and Diamond-like Nanocomposite Films *Physica Status Solidi (c)* 6 2009: pp. 2817 – 2819.

65. **Grill, A.** From Tribological Coatings to Low-k Dielectrics for ULSI Interconnects *Thin Solid Films* 398 – 399 2001: pp. 527 – 532.

66. **Goell, A., Venkatramanl, C., Dorfman, B. F., Abraizovz, M., Enge, T. G., Lote, N. G.** Diamond-like Nanocomposite Coatings Possessing High Dielectric Strength *IEEE 5th International Conference on Conduction and Breakdown in Solid Dielectrics* 1995: pp.690 – 695.

67. **Bozhko, A., Shupegin, M., Takagi, T.,** Space-charge-limited Current in Hydrogenated Amorphous Carbon Films Containing Silicon and Oxygen *Diamond and Related Materials* 11 2002: pp. 1753 – 1759.

68. **Ruiz, F., Sun, W. D., Pollak, F. H., Venkatramanl, C.** Determination of the Thermal Conductivity of Diamond-like Nanocomposite films Using a Scanning Thermal Microscope *Applied Physics Letters* 73 1998: pp.1802 – 1804.

69. **Shamsa, M., Liu, W. L., Balandin, A. A., Casiraghi, C., Milne, W. I., Ferrari, A. C.** Thermal Conductivity of Diamond-like Carbon Films *Applied Physics Letters* 89 2006: pp. 161921 (3 p.).

70. **Bullen, A. J., O'Hara, K. E., Cahill, D. G., Monteiro, O., Von Keudell, A.** Thermal Conductivity of Amorphous Carbon Thin Films *Journal of Applied Physics* 88 2000: pp. 6317 – 6320.

71. **Chen, G., Hui, P., Xu, S.** Thermal Conduction in Metalized Tetrahedral Amorphous Carbon (ta-C) Films on Silicon *Thin Solid Films* 366 2000: pp. 95 – 99. http://dx.doi.org/10.1016/S0040-6090(99)01097-4

72. **Kim, T.-Y., Ingmar, B., Bewilogua, K., Oh, K. H., Lee, K.-R.** Wetting Behaviours of a-C:H:Si:O Film Coated Nano-scale Dual Rough Surface *Chemical Physics Letters* 436 2007: pp. 199 – 203. http://dx.doi.org/10.1016/j.cplett.2007.01.036

73. **Yun, Y., Yoshida, T., Shimazu, N., Nanba, N., Inoue, Y., Saito, N., Takai, O.** Influence of Ar Gas Flow Rate in Organosilicon Plasma for the Fabrication of SiO:CH Thin Films by PECVD Method *Surface & Coatings Technology* 202 2008: pp. 5259 – 5261. http://dx.doi.org/10.1016/j.surfcoat.2008.06.004

74. **Meškinis, Š., Tamulevičius, S., Kopustinskas, V., Gudonytė, A., Grigaliūnas, V., Jankauskas, J., Gudaitis, R.** Micromachining of Diamond-like Carbon Deposited by Closed Drift Ion Source for Cantilevers and Membranes *Materials Science* (*Medžiagotyra*) 15 2009: pp. 201 – 206.

75. **Grigaliūnas, V., Tamulevičius, S., Muehlberger, M., Mittendorfer, G., Glinsner, T., Zakas, G., Meškinis, Š., Guobienė, A., Palevičius, A., Janušas, G.** Imprint Lithography for Large Scale Angular Encoders *Materials Science* (*Medžiagotyra*) 13 2007: pp. 103 – 106.

76. **Prasad, S. V., Scharf, T. W., Kotula, P. G., Michael, J. R., Christenson, T. R.** Application of Diamond-like Nanocomposite Tribological Coatings on LIGA Microsystem Parts *Journal of Microelectromechanical Systems* 18 2009: pp. 695 – 704. http://dx.doi.org/10.1109/JMEMS.2009.2016284

77. **Das, T., Ghosh, D., Bhattacharyya, T. K., Maiti, T. K.** Biocompatibility of Diamond-like Nanocomposite Thin Films *Journal of Materials Science: Materials in Medicine* 18 2007: pp. 493 – 500. http://dx.doi.org/10.1007/s10856-007-2009-x

78. **De Scheerder, I., Szilard, M., Yanming, H., Ping, X. B., Verbeken, E., Neerinck, D., Demeyere, E., Coppens, W., Van de Werf, F.** Evaluation of the Biocompatibility of Two New Diamond-like Stent Coatings (Dylyn) in a Porcine Coronary Stent Model *The Journal of Invasive Cardiology* 12 2000: pp. 389 – 394.